

Size dependence of photoluminescence and resonant Raman scattering from ZnO quantum dots

Hsin-Ming Cheng, Kuo-Feng Lin, Hsu-Cheng Hsu, and Wen-Feng Hsieh

Citation: *Applied Physics Letters* **88**, 261909 (2006); doi: 10.1063/1.2217925

View online: <http://dx.doi.org/10.1063/1.2217925>

View Table of Contents: <http://scitation.aip.org/content/aip/journal/apl/88/26?ver=pdfcov>

Published by the [AIP Publishing](#)

Articles you may be interested in

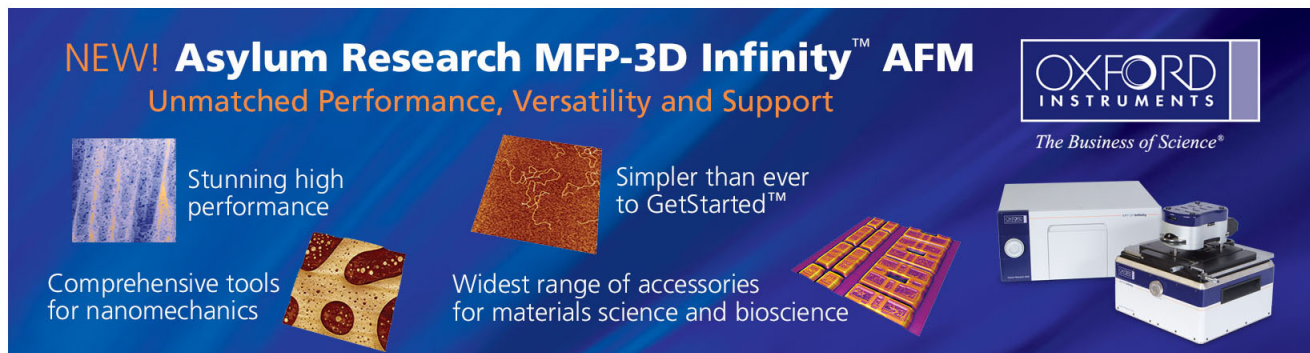
Identification of visible emission from ZnO quantum dots: Excitation-dependence and size-dependence
J. Appl. Phys. **111**, 083521 (2012); 10.1063/1.4705395

Anomalous optical processes in photoluminescence from ultrasmall quantum dots of ZnO
J. Vac. Sci. Technol. A **29**, 03A120 (2011); 10.1116/1.3578344

Size dependence of the electronic structures and electron-phonon coupling in ZnO quantum dots
Appl. Phys. Lett. **91**, 262101 (2007); 10.1063/1.2824396

Study on the quantum confinement effect on ultraviolet photoluminescence of crystalline ZnO nanoparticles with nearly uniform size
Appl. Phys. Lett. **90**, 263113 (2007); 10.1063/1.2750527

Raman scattering and photoluminescence of As ion-implanted ZnO single crystal
J. Appl. Phys. **96**, 175 (2004); 10.1063/1.1756220

The advertisement features a dark blue background with white and orange text. At the top left, it reads 'NEW! Asylum Research MFP-3D Infinity™ AFM' in large white letters, with 'Unmatched Performance, Versatility and Support' in orange below it. To the right is the Oxford Instruments logo, which includes the text 'OXFORD INSTRUMENTS' and the tagline 'The Business of Science®'. Below the main text are four images: a blue textured surface, a brown textured surface, a grid of colorful squares, and a photograph of the MFP-3D Infinity AFM instrument. Each image is accompanied by a short text description: 'Stunning high performance', 'Simpler than ever to GetStarted™', 'Comprehensive tools for nanomechanics', and 'Widest range of accessories for materials science and bioscience'.

Size dependence of photoluminescence and resonant Raman scattering from ZnO quantum dots

Hsin-Ming Cheng,^{a)} Kuo-Feng Lin, Hsu-Cheng Hsu, and Wen-Feng Hsieh^{b)}
*Department of Photonics and Institute of Electro-Optical Engineering, National Chiao Tung University,
 1001 Tahsueh Road, Hsinchu 30050, Taiwan, Republic of China*

(Received 17 March 2006; accepted 24 May 2006; published online 28 June 2006)

ZnO quantum dots (QDs) of controlled sizes have been fabricated by a simple sol-gel method. The blueshift of room-temperature photoluminescence measurement from free exciton transition are observed decreasing with the QD size that is ascribed to the quantum confinement effect. From the resonant Raman scattering, the coupling strength between electron and longitudinal optical phonon, deduced from the ratio of the second- to the first-order Raman scattering intensity, diminishes with reducing the ZnO QD diameter. The size dependence of electron-phonon coupling is principally a result of the Fröhlich interaction. © 2006 American Institute of Physics. [DOI: 10.1063/1.2217925]

ZnO is a promising material for short-wavelength photonic devices since it has a large direct band gap of 3.37 eV, and a large exciton binding energy of 60 meV, all of which are advantageous for light-emitting diode and low-threshold optical pumped laser applications at room temperature. For the feasible requirement, low-dimensional ZnO nanostructures, such as quantum dots (QDs),^{1,2} nanoparticles (NPs),^{3,4} nanobelts,⁵ nanowires,⁶ and quantum wells,⁷ have been widely investigated. In particular, ZnO QDs and NPs are of great interest because of the three-dimensional confinement of carrier and phonon leads not only continuous tuning of the optoelectronic properties but also improvement in device performance. Recently, Demangeot *et al.*⁴ have reported the resonant Raman scattering (RRS) and low-temperature photoluminescence (PL) from ZnO NPs with different particle sizes which were synthesized by a room-temperature organometallic method. However, the study showed no size effects from the aspect of either carrier or phonon. The origin of weak size dependence of longitudinal optical (LO) phonon frequency was explained by the ligands bonded to the particle surface, and no shift from the low-temperature PL measurement indicated that UV emission was most likely dominated by weakly bound localized defects, which could come from the surface-bound ionized acceptor-exciton complexes, rather than the size-dependent quantum confinement effect. It is therefore important to note that the nanocrystals synthesized by chemical methods indeed occasionally cause the product suffering the active surround, such as ligands, which could intensely transform the intrinsic properties of the core. Accordingly, the demand for surface passivation of the NPs and the QDs is significant from both the fundamental scientific research and photonic application points of view. In this letter, we demonstrate the size-dependent PL and RRS of ZnO QDs which are fabricated by a simple sol-gel method without placing any ligands. The enlargement of free exciton transition energy is responsible for the blueshift of near-band-edge emission in ZnO QDs at room temperature. Moreover, the size dependence of electron-phonon coupling, which can be addressed principally as a result of the Fröhlich

interaction, is confirmed by resonant Raman spectra.

The ZnO QDs were synthesized via a simple sol-gel method without placing any ligands. The average size can be tailored by the concentration of precursor, zinc acetate dihydrate [99.5% Zn(OAc)₂, Riedel-deHaen]. A high speed centrifuge was used to separate the final colloids into the upper suspension and the white bottom layer, which include the monodispersed single crystalline ZnO QDs and the secondary ZnO clusters, respectively. In this present work, we considered only the monodispersed ZnO QDs to avoid the intricately mutual interaction. Additional detail of the synthesis can be found elsewhere.⁸ The microstructures were analyzed by JEOL JEM-2100F field emission transmission electron microscope (FETEM) operated at 200 KeV. The phase and average crystallite size were characterized using Bede D1 thin film x-ray diffractometer (TFXRD). Resonant Raman spectroscopy was carried out by a He-Cd laser ($\lambda=325$ nm), and a Jobin-Yvon T64000 microspectrometer with a 1800 grooves/mm grating in the backscattering configuration. Room-temperature PL measurements were also performed using the 20 mW He-Cd laser ($\lambda=325$ nm).

Figure 1 shows a TEM micrograph of the ZnO QDs formed using 0.06M zinc precursor. The ZnO QDs are little aggregated but still appear to be sphere and ellipsoid in shape. The mean-particle size is estimated to be ca. 4.2 nm. The electron and x-ray diffractions (not shown) all coincide with the presence of hexagonal wurzite crystallites with cell constants of $a=3.251$ Å and $c=5.208$ Å. No excess peaks are detected, which indicates that all the precursors have been completely decomposed. Blueshift of room-temperature ultraviolet (UV) emission was investigated in a series of ZnO QDs with different average sizes, as shown in Fig. 2(a). The broad shape of PL peaks is apparently due to the moderate size distribution of ZnO QDs. The nature of the UV-PL from ZnO QDs itself is still a matter of controversy.¹ Aforementioned Demangeot *et al.*⁴ have reported that ligands coordinated at the surface of the nanoparticles may induce some changes in ZnO bonds, leading to some modifications of either their mechanical or dielectric properties. The UV-PL that came from surface-bound ionized acceptor-exciton complexes revealed no significant energy shift with varying size of ZnO NPs; furthermore, the weak bound emission vanished at the measured temperature higher than 15 K. In contrast, in

^{a)} Also at: Material and Chemical Research Laboratories, Industrial Technology Research Institute, Hsinchu 310, Taiwan, Republic of China.

^{b)} Author to whom correspondence should be addressed; electronic mail: wfhsieh@mail.nctu.edu.tw

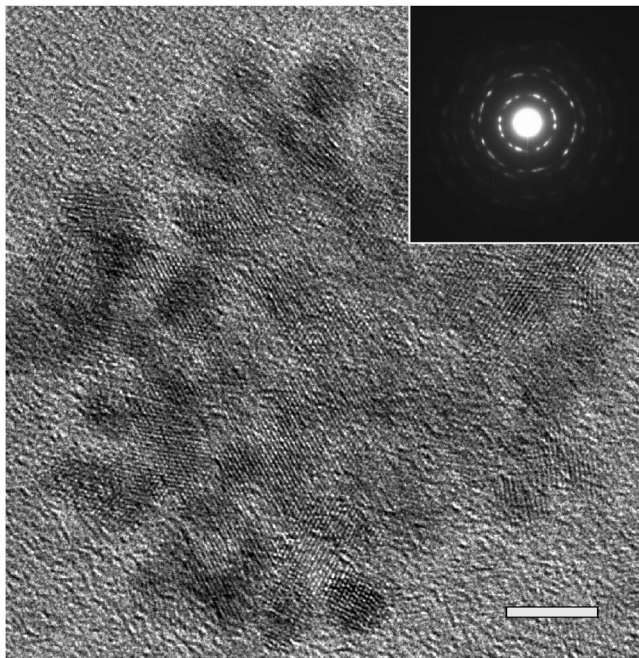


FIG. 1. TEM image of the ZnO QDs fabricated using 0.06M precursor with the inset of its corresponding selected area electron diffraction (SAED) pattern. The scale bar has a length of 5 nm.

the present work, the relaxed state near the band edge is attributed to the free exciton emission with high electronic density of states because no ligands were added during our synthesis process and the intense UV emission still exhibited even at room temperature. The UV emission shifts to the higher energy from 3.3 to 3.43 eV as the particle size reduces from 12 to 3.5 nm. Moreover, the discernible broad green band (2.1–2.8 eV) was observed only when the size of ZnO QDs is smaller than 4.2 nm as shown in Fig. 2(b), the surface-located complex emission reasonably be enhanced while the surface volume of QDs were increased as decreasing the particle size. The relatively weak visible emission indicated that the ZnO QDs contain less intrinsic defects at the surface. Since the exciton Bohr radius a_B of bulk ZnO is 2.34 nm,⁹ the carrier confinement in these ZnO QDs are in

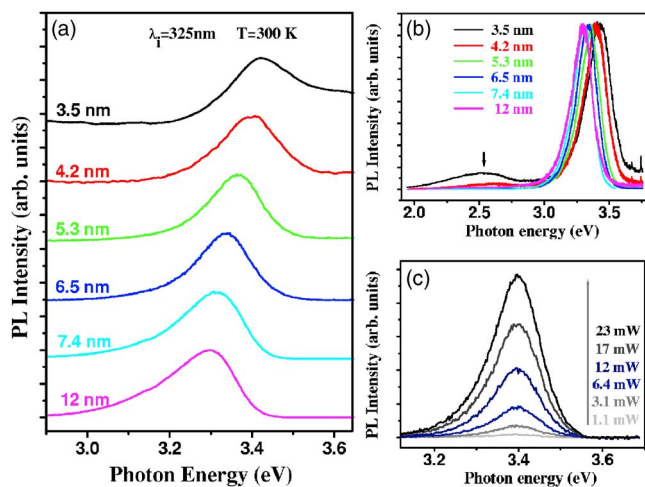


FIG. 2. (Color online) Room-temperature PL spectra (a) and green emission (b) of ZnO QDs with various sizes. (c) PL spectra of ZnO QDs (4.2 nm in diameter) as a function of excitation laser intensity (from 1.1 to 23 mW). The exponent γ of power law $I \sim L^\gamma$ lies about 1.3.

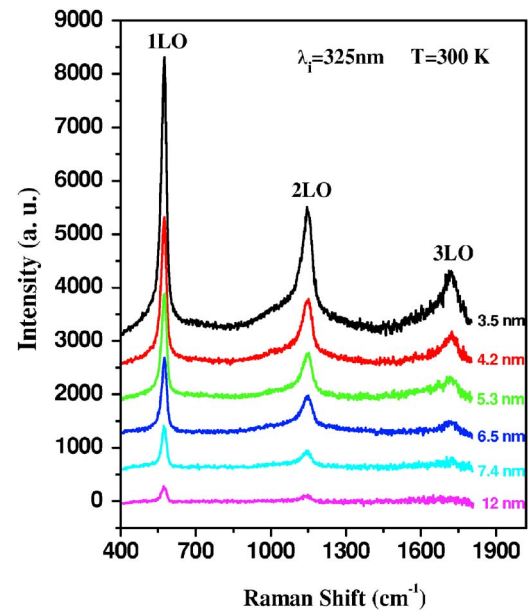


FIG. 3. (Color online) Resonant Raman scatterings of ZnO QDs with various particle sizes measured at room temperature using a He-Cd laser ($\lambda = 325$ nm).

the moderate to strong confinement regimes. The enlarged band gap from 3.41 to 3.60 eV as the ZnO QD size reduces from 12 to 3.5 nm has been estimated by effective mass model in our previous study.⁸ Although the energy differences come from the relaxed state of the exciton and its binding energy, the parallel tendency consists with our assumption of quantum confinement effect. To circumvent other probabilities, we operated the PL measurements at different power. The unchanged energies of the UV emission peaks, as shown in Fig. 2(c), exhibit no considerable local heating effect in ZnO QDs, and the obtained exponent value about 1.3 of power law confirmed our assignment that the observed UV emission bands are due to excitonic transition.

The electron-phonon interaction could be straightly probed by the RRS when the exciting photon energy is resonant with the electronic interband transition energy of the wurtzite ZnO. The polar symmetry makes the $A_1(\text{LO})$ and $E_1(\text{LO})$ modes the dominant ones, while the nonpolar E_2 phonon is not visible. An intense multiphonon scattering of the ZnO QDs with various sizes was observed in the resonant Raman spectra of Fig. 3 with background subtracted, where three major bands were observed to result mainly from the polar symmetry modes $A_1(\text{LO})$ and $E_1(\text{LO})$ and their overtones. Multiphonon scattering processes that have been previously reported for one-dimensional (1D), two-dimensional (2D), and three-dimensional (3D) ZnO systems,^{10–14} in particular, have been recently reported intensely for zero-dimensional (0D) systems.^{2,4,15}

It is remarkable that the intensities of the first-order Raman modes and their overtones are enhanced while the size of ZnO QDs decreases. The reason can be explained using the total Raman cross section for an n -phonon process as a result of the energy of the incoming or the scattered photon that matches real electronic states in the material to enhance the Raman scattering cross section. The band gap of the present ZnO QDs certainly tends to approach the excitation laser energy as decreasing its size because of the quantum-confined effect mentioned above. Alim *et al.*¹⁶ have shown

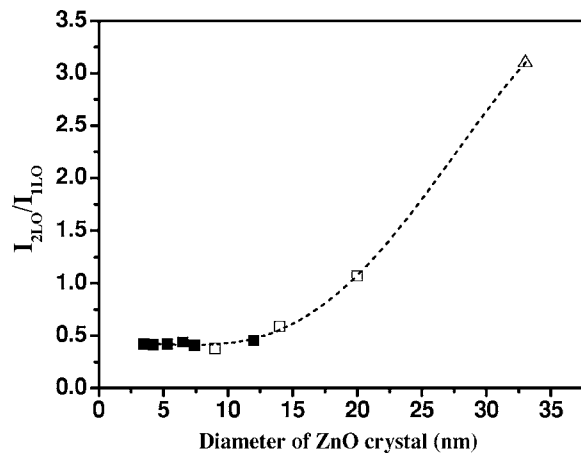


FIG. 4. Ratio between the second- and the first-order Raman scattering cross sections as a function of ZnO diameter. The experimental values of ZnO QDs in this work (squares) compared with ZnO NPs of Ref. 15 (empty squares) and nanocrystalline ZnO thin films of Ref. 11 (empty triangle). The dashed line joining the data points is just a guide for the eyes.

that the large redshifts in the RRS spectra from 20 nm ZnO QDs are most likely due to the local heating by UV laser excitation. In the present RRS spectra, the 1LO frequencies were all located at $\sim 575 \text{ cm}^{-1}$ (within $\pm 2 \text{ cm}^{-1}$ fluctuation) for the ZnO QDs of different sizes. The heating effect coming from the inspection of micro-Raman seems to be negligible, because we used the laser power of only 0.8 mW at the spot size about $100 \mu\text{m}^2$.

Beyond the phonon frequency shift, by observing the size dependence of intensity ratio between the second- and the first-order LO Raman scatterings, one can evaluate the coupling strength of the electron-phonon interaction. Within the Franck-Condon approximation,¹⁶ the electronic oscillation strength distribution over n th phonon mode is defined as $I \sim S^n e^{-S}/n!$, in which S is Huang-Rhys parameter, and also can be used to express the coupling strength of the electron to the LO phonon. The ratio between the second- and the first-order Raman scattering cross sections was found to increase remarkably from 0.4 to 3.1 while an increase of the ZnO crystallite size was from 3.5 to 33 nm, as shown in Fig. 4.

The electron-phonon coupling is generally determined by two mechanisms: the deformation potential and the Fröhlich potential. On the one hand, following Loudon¹⁷ and Kaminow and Johnston,¹⁸ the transverse optical (TO) Raman scattering cross section is determined by the deformation potential that involves the short-range interaction between the lattice displacement and the electrons, and on the other, the LO Raman scattering cross section includes contributions from both the deformation potential and Fröhlich potential that involves the long-range interaction generated by the

macroscopic electric field associated with the LO phonons. We found that under the resonant conditions the intensity of TO phonon in ZnO QDs is almost insensitive, while that of LO phonon is greatly enhanced. Therefore, we believe that the electron-phonon coupling as decreasing the nanocrystal size is mainly associated with the Fröhlich interaction. Although the complex origin of coupling is not well understood, the result in this study is extremely consistent with reports in other low-dimensional ZnO nanosystems.^{7,19,20}

In summary, the enlarged free-exciton transition energy is responsible for the blueshift of near-band-edge PL spectra in ZnO QDs and gives significant evidence for the quantum confinement effect. Moreover, an increasing electron-phonon coupling was also discovered from RRS analysis while the diameter of ZnO crystal increases. The size dependence of electron-phonon coupling is principally as a result of the Fröhlich interaction.

Research supported by the National Science Council (NSC) (Project No. NSC-94-2112-M-009-015) and the Nano Technology Research Center (NTRC/ITRI) (Project No. A341XSYM91) in Taiwan.

- ¹V. A. Fonoberov and A. Balandin, *Appl. Phys. Lett.* **85**, 5971 (2004).
- ²K. A. Alim, V. A. Fonoberov, and A. Balandin, *Appl. Phys. Lett.* **86**, 053103 (2005); K. A. Alim, V. A. Fonoberov, M. Shamsa, and A. Balandin, *J. Appl. Phys.* **97**, 124313 (2005).
- ³L. Guo, S. Yang, C. Yang, P. Yu, J. Wang, W. Ge, and G. K. L. Wang, *Appl. Phys. Lett.* **76**, 2901 (2000).
- ⁴F. Demangeot, V. Paillard, P. M. Chassaing, C. Pagès, M. L. Kahn, A. Maissonnat, and B. Chaudret, *Appl. Phys. Lett.* **88**, 071921 (2006).
- ⁵Z. W. Pan, Z. R. Dai, and Z. L. Wang, *Science* **291**, 1947 (2001).
- ⁶M. H. Huang, S. Mao, H. Feick, H. Yan, Y. Wu, H. Kind, E. Weber, R. Russo, and P. Yang, *Science* **292**, 1897 (2001).
- ⁷T. Makino, C. H. Chia, N. T. Tuan, H. D. Sun, Y. Segawa, M. Kawasaki, A. Ohtomo, K. Tamura, and H. Koinuma, *Appl. Phys. Lett.* **77**, 975 (2000).
- ⁸K. F. Lin, H. M. Cheng, H. C. Hsu, L. J. Lin, and W. F. Hsieh, *Chem. Phys. Lett.* **409**, 208 (2005).
- ⁹R. T. Senger and K. K. Bajaj, *Phys. Rev. B* **68**, 045313 (2003).
- ¹⁰J. F. Scott, *Phys. Rev. B* **2**, 1209 (1970).
- ¹¹X. T. Zhang, Y. C. Liu, Z. Z. Zhi, J. Y. Zhang, Y. M. Lu, D. Z. Shen, W. Xu, G. Z. Zhong, X. W. Fan, and X. G. Kong, *J. Phys. D* **34**, 3430 (2001).
- ¹²V. V. Ursaki, I. M. Tiginyanu, V. V. Zalamai, V. M. Masalov, E. N. Samarov, G. A. Emelchenko, and F. J. Briones, *J. Appl. Phys.* **96**, 1001 (2004).
- ¹³H. T. Ng, B. Chen, J. Li, J. Han, M. Meyyappan, J. Wu, S. X. Li, and E. E. Haller, *Appl. Phys. Lett.* **82**, 2023 (2003).
- ¹⁴H. M. Cheng, H. C. Hsu, Y. K. Tseng, L. J. Lin, and W. F. Hsieh, *J. Phys. Chem. B* **109**, 8749 (2005).
- ¹⁵H. M. Cheng, K. F. Lin, H. C. Hsu, C. J. Lin, L. J. Lin, and W. F. Hsieh, *J. Phys. Chem. B* **109**, 18385 (2005).
- ¹⁶K. Huang and A. Rhys, *Proc. R. Soc. London, Ser. A* **204**, 406 (1950).
- ¹⁷R. Loudon, *Adv. Phys.* **13**, 23 (1964).
- ¹⁸I. P. Kaminow and W. D. Johnston, *Phys. Rev.* **160**, 19 (1967).
- ¹⁹T. Makino, K. Tamura, C. H. Chia, Y. Segawa, M. Kawasaki, A. Ohtomo, and H. Koinuma, *Phys. Rev. B* **66**, 233305 (2002).
- ²⁰R. P. Wang, G. Xu, and P. Jin, *Phys. Rev. B* **69**, 113303 (2004).